

# Two-Way Molecular Communications

Jong Woo Kwak, *Student Member, IEEE*, H. Birkan Yilmaz, *Member, IEEE*, Nariman Farsad, *Member, IEEE*, Chan-Byoung Chae, *Senior Member, IEEE*, and Andrea Goldsmith, *Fellow, IEEE*

**Abstract**—For nano-scale communications, there must be cooperation and simultaneous communication between nano devices. To this end, in this paper we investigate two-way (a.k.a. bi-directional) molecular communications between nano devices. If different types of molecules are used for the communication links, the two-way system eliminates the need to consider self-interference. However, in many systems, it is not feasible to use a different type of molecule for each communication link. Thus, we propose a two-way molecular communication system that uses a single type of molecule. We develop a channel model for this system and use it to analyze the proposed system’s bit error rate, throughput, and self-interference. Moreover, we propose analog- and digital- self-interference cancellation techniques. The enhancement of link-level performance using these techniques is confirmed with both numerical and analytical results.

**Index Terms**—Molecular communication, two-way communication, and self-interference cancellation.

## I. INTRODUCTION

OVER the past decade, developments in the field of nanorobotics have enabled the use of nano devices in various technologies and especially in those used by the bio-medical industry [1]–[5]. Well-organized clusters of nano devices can be used for drug delivery applications and artificial immune systems. Each cluster is responsible for a single task, say, for example, discovering or destroying of pathogens. Since a nano device can only perform simple tasks, it is important to have a communication system among nano devices. Radio frequency (RF)-based communication is not suitable for nano devices because of physical limitations such as the size of the antenna, which is typically proportional to the wavelength of the electromagnetic (EM) wave in order to maximize efficiency [6], [7]. Furthermore, EM waves—especially at high frequencies—do not propagate well in the body [8].

Thus, researchers have focused on molecular communication as an alternative to RF-based communication, where information is transmitted via molecules. One such system is that of molecular communication via diffusion (MCvD). Here molecules are propagated in an environment by diffusion [9]. An MCvD system mainly consists of the following: a transmitter node capable of emitting and modulating information

through molecules, a receiver node capable of receiving and demodulating molecular signals, information molecules to transfer information, and a fluid environment to host nodes and molecules.

One of the main challenges in MCvD is to establish channel models for representing the molecular received signal (i.e., the fraction of received molecules until time  $t$ ). Some known channel models assume that the arrival time of molecules are a first-passage time process (i.e., information molecules are absorbed whenever they hit a receiver) [10]–[14]. When the time of arrival in an MCvD system is modeled by a first-passage process, each molecule can contribute to the molecular received signal only once. The authors in [13] modeled the molecular received signal in a three-dimensional (3-D) environment— a point source represented a transmitter, and an absorbing sphere represented a receiver. Regarding this basic topology, it is possible to acquire an analytical closed form of the channel model representing the molecular received signal due to spherical symmetry. If the system has more than one absorbing sphere (receiver), however, such symmetry disappears. It then difficult to model the arrival times mathematically.

Other challenges in MCvD include low transmission rates due to severe inter-symbol interference (ISI). In MCvD, ISI occurs when the molecules of a previous symbol are absorbed by the target receiver in the current or future symbol slots. The heavy tail nature of impulse responses in MCvD causes severe ISI. Thus, several researchers [15]–[17] have suggested ISI mitigation techniques, including enzymatic degradation of ISI using different molecule types. All of these works assumed an one-way MCvD system whereby molecules are transmitted in one direction from the transmitter to the receiver. While this simplifies the design, recent work in full-duplex radio communications indicates that data rate gains along with other performance advantages may be obtained from two-way communication.

In this paper, we propose a two-way MCvD system that uses a *single* type of molecule for simultaneous communication between two nano devices. If each of the directional communication links uses a different type of molecule, then self-interference<sup>1</sup> (SI) will not occur and the problem becomes trivial [18], [19]. However, this is not a feasible solution. First, the nano devices are too simple to perform complex tasks and, second, the number of molecule types will increase rapidly, on the order of  $\binom{\ell}{2}$  where  $\ell$  is the number of communication links. Therefore, we propose a two-way MCvD system that uses a single type of molecule for each link. However, the analytical

J. Kwak and C.-B. Chae are with the School of Integrated Technology, Yonsei University, Korea. H. B. Yilmaz was with the School of integrated Technology, Yonsei University, Korea, and now he is with the Dept. of Network Engineering, Polytechnic University of Catalonia, Spain. N. Farsad and A. Goldsmith are with the Department of Electrical Engineering, Stanford University, USA.

This research was supported in part by the MSIT (Ministry of Science and ICT), Korea, under the ICT Consilience Creative program (IITP-2017-2017-0-01015), the Basic Science Research Program (2017R1A1A1A05001439) through the National Research Foundation of Korea, the Government of Catalonia’s Secretariat for Universities and Research via the Beatriu de Pinós postdoctoral program, and the NSF Center for Science of Information (CSol) under grant CCF-0939370.

<sup>1</sup>Self-interference in MCvD refers to a phenomenon in which a molecule emitted from the transmitter is absorbed by its own rather than the intended receiver.

modeling of such a system is not without difficulty—two absorbing spheres are to use a single type of molecule. Unfortunately, to implement simultaneous communication between two nano devices, we cannot use previous studies on MCvD channel models as such studies assumed an one-way MCvD system with a single absorbing sphere. Therefore, in this paper, we analytically model the molecular received signal in the case of two absorbing spheres, propose SI cancellation (SIC) techniques, and analyze the proposed system's performance in terms of bit error rate (BER) and throughput. The main contributions of this paper are as follows:

- The impulse response of a two-way MCvD system that uses a single type of molecule for each link is investigated. Two communication models—a half-duplex system and a full-duplex system—are considered. In the half-duplex system, each paired transceiver operates alternately with respect to time. In the full-duplex system, each paired transceiver operates simultaneously with respect to time (i.e., it is not necessary to wait until the other transceiver ends its communication).
- The paper derives the BER expression for two two-way MCvD systems—one with a half-duplex system and one with a full-duplex system. The theoretical BERs are then validated through simulations.
- The paper proposes two SIC techniques—analogue SI cancellation (ASIC) and digital SI cancellation (DSIC)—as analytical results show that it is impossible to achieve reliable data transmission without SIC in the full-duplex system.
- The existence of optimal values for the normalized detection threshold and the time after which molecules are discarded period in order to minimize the BER of the two considered two-way MCvD systems is confirmed through theoretical analyses; the optimal values for these parameters are then approximated numerically as a closed-form solution for them could not be obtained.

The rest of this paper is organized as follows. In Section II, we discuss the conventional one-way MCvD model. In Section III, we introduce the proposed two-way MCvD system and SIC techniques. In Section IV, we present channel model verifications and BER formulations for the two considered systems. In Section V, we present performance analysis results in terms of BER and throughput for the two considered systems. Finally, in Section VI, we present our conclusions.

## II. ONE-WAY MOLECULAR COMMUNICATION

We start by providing details of the conventional model for one-way MCvD. Also, we present details of the relevant channel model so that the reader may understand the differences and challenges with respect to the corresponding model for two-way molecular communication system.

### A. Conventional model

The conventional model for one-way MCvD system consists of a point source (point transmitter) and an absorbing sphere (receiver). In Fig. 1, the point source (point transmitter), Tx, is separated from the absorbing sphere (receiver), Rx<sub>1</sub>, the

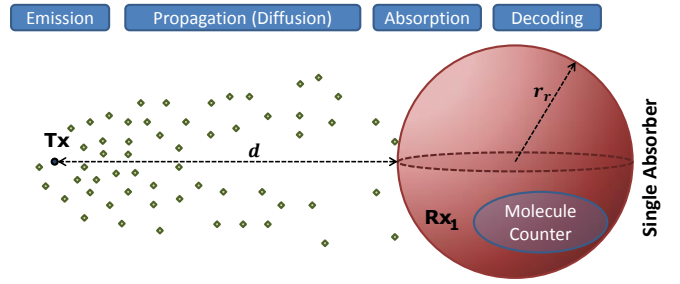


Fig. 1. Conventional model for one-way MCvD and the processes with a point transmitter (Tx) and an absorbing sphere (Rx<sub>1</sub>).

radius of which is denoted by  $r_r$ , by a distance of  $d$ . Here we focus on three molecular processes: emission, propagation, and reception. The emission process is related to the modulation of the data bits onto the physical properties of the molecules or the emission time [20]. The propagation process is governed by diffusion and flow [21]–[23]. The reception process is related to the acquisition of the molecules at the receiver and the demodulation of the data bits.

Regarding the propagation process, the interactions between diffusing molecules are ignored since the messenger molecules are assumed to be chemically stable. Also assume that the transmitter and the receiver are fully synchronized, which can be achieved by the method introduced in [24].

### B. Channel Model for One-way Molecular Communication with a Single Receiver

In diffusion-based systems, molecules tend to move towards the less concentrated areas, which means that the derivative of the flux with respect to time results in Fick's second law in a 3-D environment; that is

$$\frac{\partial p(r, t|r_0)}{\partial t} = D\nabla^2 p(r, t|r_0), \quad (1)$$

where  $\nabla^2$ ,  $p(r, t|r_0)$ , and  $D$  are the Laplacian operator, the molecule distribution function at time  $t$  and distance  $r$  given the initial distance  $r_0$ , and the diffusion constant, respectively. The value of  $D$  depends on the temperature, viscosity of the fluid, and the Stokes radius of the molecule.

Fig. 1 illustrates a simple topology of one-way MCvD. In [13], the expected channel response of one-way MCvD is presented and analyzed from a channel characteristics perspective. Also, a time-dependent solution for a fraction of molecules hitting a single absorbing sphere (Rx<sub>1</sub>) until time  $t$  is presented, as follows:

$$\begin{aligned} G_1^{\text{Tx}}(t) &= \int_0^t g_1^{\text{Tx}}(t') dt' \\ &= \int_0^t \frac{r_r}{r_r + d} \frac{d}{\sqrt{4\pi Dt'^3}} e^{-d^2/4Dt'} dt' \\ &= \frac{r_r}{r_r + d} \operatorname{erfc}\left(\frac{d}{\sqrt{4Dt}}\right), \end{aligned} \quad (2)$$

where  $g_1^{\text{Tx}}(t)$ ,  $r_r$ ,  $d$ , and  $\operatorname{erfc}(\cdot)$  represent the instantaneous hitting probability density (i.e., the arrival time distribution

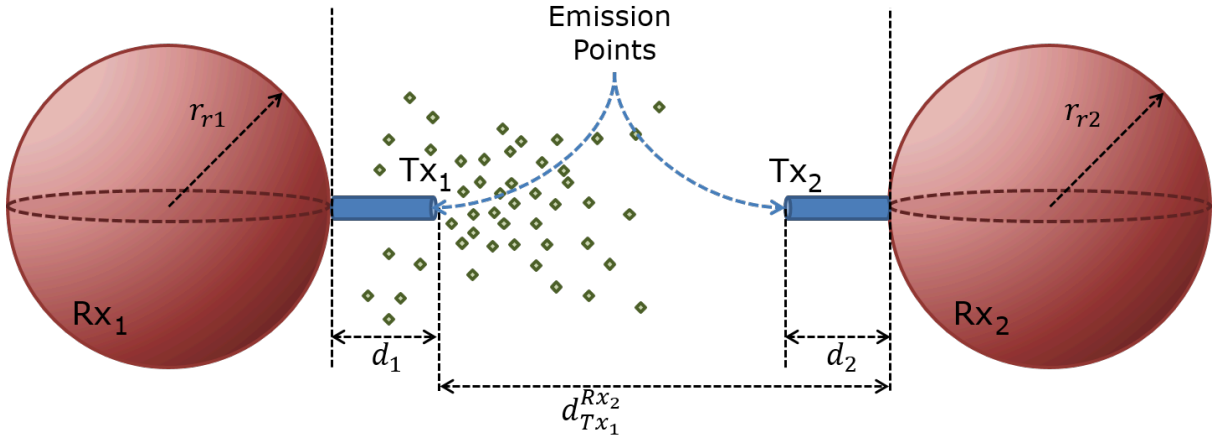


Fig. 2. Model for two-way MCvD system featuring two transmitters (i.e.,  $Tx_1$  and  $Tx_2$ ) and two receivers (i.e.,  $Rx_1$  and  $Rx_2$ ).

for  $Rx_1$ ), the radius of the receiver, the distance from  $Tx$  to  $Rx_1$ , and the complementary error function, respectively.

### III. TWO-WAY MOLECULAR COMMUNICATION

In this section, we introduce two modes of operation for the proposed two-way MCvD system, i.e., full-duplex and half-duplex based on time-division. In the former case, severe SI is observed when both transceivers simultaneously modulate signals using the same type of molecule. Therefore, in this case, it is necessary to apply an SIC technique.

#### A. Topology

We consider a 3-D environment with two point sources (transmitters) and two absorbing spheres (receivers). Each transmitter emits molecules without directionality. The molecules are immediately absorbed when they reach the surface of any one of the receivers. Since the absorbed molecules are removed from the system, each molecule is detected at most once.

Fig. 2 shows the model of the proposed system.  $Tx_i$  releases molecules that are intended to be absorbed by  $Rx_j$  ( $i \neq j$ ). If the molecules that are released from  $Tx_i$  are absorbed by  $Rx_i$  (not the desired result), then we call this SI. The distance between  $Tx_i$  and  $Rx_i$  is denoted by  $d_i$ , and the shortest distance between a point  $p$  and the surface of  $Rx_j$  is denoted by  $d_p^{Rx_j}$ .

#### B. Communication Model & Modulation

Consider the following two modes of operation for the proposed two-way MCvD system:

- Half-duplex system:  $Tx_i$  and  $Tx_j$  release molecules alternately (i.e., when  $Tx_i$  emits molecules,  $Rx_i$  and  $Rx_j$  receive the molecules but  $Rx_i$  does not count the molecules).
- Full-duplex system:  $Tx_i$  and  $Tx_j$  release molecules simultaneously that are intended for  $Rx_j$  and  $Rx_i$ , respectively. Receiver  $Rx_i$  receives and counts the molecules that are

emitted by  $Tx_i$  and intended for  $Rx_j$  and similarly for  $Rx_j$ .

In the half-duplex system, at least half of the elements of the bit sequences are not used (i.e., there is no emission at the relevant symbol slots), which is not the case for the full-duplex system. Therefore, the ISI and the SI are much more severe in the full-duplex system. For the  $n^{\text{th}}$  symbol period, the molecular received signal is composed of  $2n$  bits including the current symbols and the previous  $2n-2$  symbols sent from the two transmitters. The bit sequences for the transmitters are denoted by  $x_1[1:n]$  and  $x_2[1:n]$ .

For the modulation, we use binary/quadrature concentration shift keying (BCSK, QCSK) [20], [25]. We let  $N_1$  denote the number of molecules for encoding bit-1, and we define that there will be no emission in the case of bit-0 for BCSK. Each of the transmitters has its bit sequences  $x_i$  to encode, where  $x_i[k]$  denotes the symbol in the  $k^{\text{th}}$  symbol duration for  $Tx_i$ . We define  $P_{ij}[k]$  as the probability that molecules emitted from  $Tx_i$  hit  $Rx_j$  in the  $k^{\text{th}}$  symbol duration after the emission, which is formulated as follows:

$$P_{ij}[k] \triangleq P_{ij}(kt_s, (k+1)t_s), \quad k \in \mathbb{N}_0, \quad (3)$$

where  $t_s$  and  $P_{ij}(t_1, t_2)$  denote the symbol duration and the probability that molecules emitted from  $Tx_i$  are absorbed by  $Rx_j$  but not  $Rx_i$  between time  $t_1$  and  $t_2$  after the emission.

In (3),  $P_{ij}[0]$  indicates the probability of being absorbed in the current symbol slot. We let  $y_{Rx_j}[n]$  denote the number of molecules that are absorbed by  $Rx_j$  in the  $n^{\text{th}}$  symbol slot. Note that  $y_{Rx_j}[n]$  can be affected by the number of molecules released from (i) a pair source at the current symbol slot, (ii) a pair source at the previous time slots, (iii) a non pair source at the current symbol slot, and (iv) non pair source at the previous time slots. To formulate  $y_{Rx_j}[n]$ , we define  $N_{ij}[k]$  as follows:

$$N_{ij}[k] \sim \mathcal{B}(N_1, P_{ij}[k]), \quad (4)$$

where  $\mathcal{B}(m, p)$  is a binomial distribution with  $m$  trials and success probability  $p$ . Then,  $y_{Rx_j}[n]$  can be formulated as

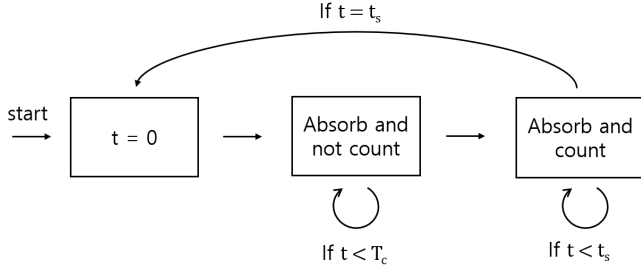


Fig. 3. State diagram of the process of ASIC. For each symbol slot, the absorbed molecules are discarded until  $t = T_c$ .

follows:

$$y_{\text{Rx}_j}[n] \triangleq \sum_{k=0}^{n-1} (N_{ij}[k] \cdot x_i[n-k] + \underbrace{N_{jj}[k] \cdot x_j[n-k]}_{\text{self-interference}}) + n_j[n]. \quad (5)$$

To consider the misoperations of the receiver, we add the noise term  $n_j[n]$  which is assumed to be a Gaussian distribution  $\mathcal{N}(0, \sigma_{\text{noise}}^2)$ . For the sake of tractability, we approximate the binomial distribution as follows [26]:

$$N_{ij}[k] \approx \mathcal{N}(N_1 P_{ij}[k], N_1 P_{ij}[k](1 - P_{ij}[k])), \quad (6)$$

where  $\mathcal{N}(\mu, \sigma^2)$  represents a Gaussian distribution with mean  $\mu$  and variance  $\sigma^2$ . Hence,  $y_{\text{Rx}_j}[n]$  can be expressed as follows (i.e., as a Gaussian random variable, where mean and variance values are dependent upon transmitted bit sequences):

$$\begin{aligned} y_{\text{Rx}_j}[n] &\sim \mathcal{N}(\mu_{\text{total}}, \sigma_{\text{total}}^2) \\ \mu_{\text{total}} &= \sum_{k=0}^{n-1} N_1 (P_{ij}[k] x_i[n-k] + P_{jj}[k] x_j[n-k]) \\ \sigma_{\text{total}}^2 &= \sigma_{\text{noise}}^2 + \sum_{k=0}^{n-1} N_1 (P_{ij}[k](1 - P_{ij}[k]) x_i[n-k] \\ &\quad + P_{jj}[k](1 - P_{jj}[k]) x_j[n-k]). \end{aligned} \quad (7)$$

### C. Self-Interference Cancellation

Since the proposed two-way MCvD system comprises two transceivers that use the same type of molecule, the system's receivers are unable to distinguish molecules in terms of the transmitting source. For example, if  $\text{Tx}_1$  sends bit-1 and  $\text{Tx}_2$  sends bit-0, the molecules are released only from  $\text{Tx}_1$ . However, those molecules can also be absorbed by  $\text{Rx}_1$ , which is not desired. Then  $\text{Rx}_1$  may decode the received signal as bit-1, even though its paired transmitter  $\text{Tx}_2$  sends bit-0. In fact, most of the molecules released from  $\text{Tx}_1$  will be absorbed by  $\text{Rx}_1$  because  $\text{Tx}_1$  is much closer to  $\text{Rx}_1$  than  $\text{Rx}_2$ . Hence, in this case, the number of received molecules is mostly dependent on the transmitted symbol from the unpaired transmitter, which makes for infeasible communication. Therefore, we propose the following two SIC techniques:

- ASIC: the initial part (i.e., between time 0 and  $T_c$ ) of the molecular received signal for each symbol slot is ignored (see Fig. 3 for the state diagram).

- DSIC: we predict the number of SI molecules (i.e., the number of absorbed molecules originating from the unpaired transmitter) from the current bit and subtract it from the molecular received signal

Fig. 4 shows the full-duplex system with ASIC and DSIC. The channel coefficients of the system with ASIC are given as follows:

$$\varphi(P_{ij}[k]) = P_{ij}(kt_s + T_c, (k+1)t_s). \quad (8)$$

Hence,  $N_{ij}[k]$  of the proposed two-way MCvD system with ASIC is denoted by  $N_{ij}^\varphi[k]$  and becomes

$$N_{ij}^\varphi[k] \sim \mathcal{B}(N_1, \varphi(P_{ij}[k])). \quad (9)$$

Furthermore,  $y_{\text{Rx}_j}[n]$  with ASIC and DSIC becomes

$$\begin{aligned} y_{\text{Rx}_j}^\varphi[n] &\triangleq \sum_{k=0}^{n-1} (N_{ij}^\varphi[k] \cdot x_i[n-k] + \underbrace{N_{jj}^\varphi[k] \cdot x_j[n-k]}_{\text{self-interference}}) \\ &\quad - \underbrace{\mathbb{E}[N_{jj}^\varphi[0] \cdot x_j[n]]}_{\text{DSIC}}, \end{aligned} \quad (10)$$

where  $\mathbb{E}[\cdot]$  is the expectation operation. After applying these two SIC techniques, we derive the BER formula.

## IV. CHANNEL MODEL & BER FORMULATION OF TWO-WAY MOLECULAR COMMUNICATION

We formulate the BER as a function of detection threshold  $\tau$ , the number of molecules for encoding bit-1 ( $N_1$ ),  $P_{ij}[k]$ , and the symbol duration  $t_s$ . In this section, we first derive the channel model function to obtain the channel coefficients  $P_{ij}[k]$  or  $\varphi(P_{ij}[k])$  and then utilize these channel coefficients in the BER calculations.

### A. Channel Model

The channel model is related to the analytical derivation of the expected fraction of molecules absorbed by the receivers until time  $t$ . In the proposed two-way MCvD system, we cannot use (2) directly to derive the channel model since we have to consider the events of molecules being absorbed by each  $\text{Rx}_i$ , which are not independent of each other. The proposed BER formula and the SIC techniques are based on the channel model. However, there is no analytical closed-form solution in the literature for the case of two absorbing spherical receivers. In prior work on molecular MIMO [27], [28], researchers considered two pairs of point transmitters and fully absorbing receivers. To obtain the channel models, the authors in [27] and [28] utilized an one-way MCvD system channel model for a single receiver [13] and fitted the coefficients accordingly. The model function of the multi-receiver channel model is different from (2). Therefore, the fitting of coefficients is not a valid way to approximate the multi-receiver channel model. Hence, we propose a new approach to derive the model function of the multi-receiver case.

We derive the multi-receiver channel model by considering the possible diffusion paths in the case of a two-way MCvD system. In Fig. 5, three possible traversal paths (diffusion paths) for a molecule emitted from  $\text{Tx}_1$  are shown. Our goal is

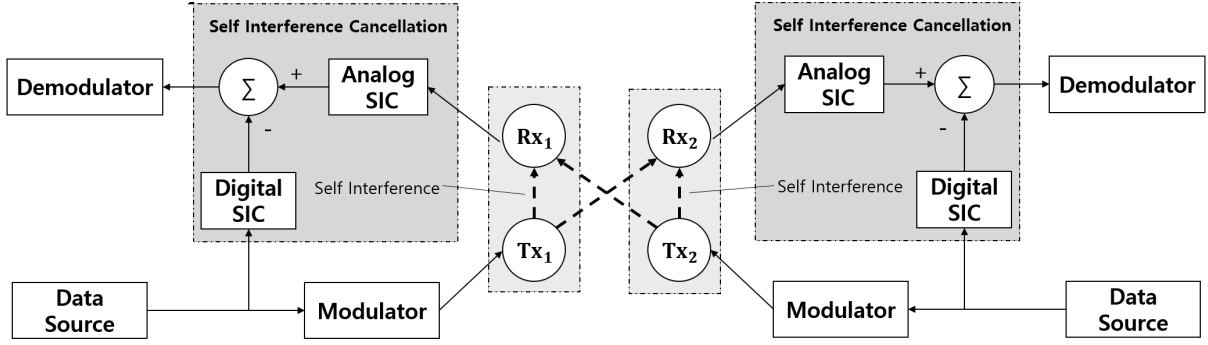


Fig. 4. Block diagram of the proposed two-way MCvD system with ASIC and DSIC.

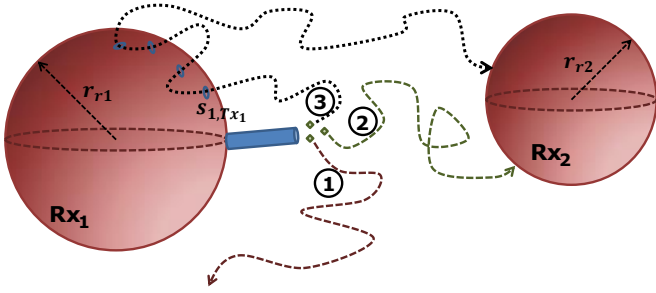


Fig. 5. Three possible traversal paths for a molecule emitted from  $Tx_1$ . Path 1 corresponds to a molecule not hitting any of the receivers until time  $t$ . Path 2 corresponds to a molecule that is hitting the destination ( $Rx_2$ ) at time  $t$  without hitting  $Rx_1$ . Path 3 is a virtual path that corresponds to a molecule that is, actually hitting  $Rx_1$  but that would hit  $Rx_2$  at time  $t$  if  $Rx_1$  was not in the environment or it was transparent to molecules.

to obtain the fraction of received molecules until time  $t$  for the receivers when  $Tx_1$  is the emitter (i.e.,  $F_1^{Tx_1}(t)$  and  $F_2^{Tx_1}(t)$  for the receivers  $Rx_1$  and  $Rx_2$ , respectively).  $F_2^{Tx_1}(t)$  can be expressed as follows:

$$F_2^{Tx_1}(t) = \int_0^t f_2^{Tx_1}(t') dt', \quad (11)$$

where  $f_2^{Tx_1}(t)$  denotes the instantaneous hitting probabilities for the molecules following Path 2. Note that  $Tx_2$  will not be considered in the derivation because we can obtain the whole case by superposition.

**Remark 1.** In the derivation of  $F_2^{Tx_1}(t)$ ,  $Rx_1$  will be regarded as a non-intended receiver on the path to  $Rx_2$  and vice versa.

**Remark 2.** To obtain the desired closed form for  $Rx_2$ , we first have to obtain the probability of the emitted molecules moving through Path 2. For this, we evaluate  $F_2^{Tx_1}(t)$  by subtracting the probability corresponding to Path 3 from the channel model of the one-way MCvD with a single point transmitter.

Hence, we consider the instantaneous hitting probability densities for  $Rx_2$  as follows:

$$f_2^{Tx_1}(t) = g_2^{Tx_1}(t) - \alpha(t), \quad (12)$$

where  $\alpha(t)$  corresponds to the instantaneous hitting probabilities for the molecules following Path 3. Additionally,  $g_2^{Tx_1}(t)$

corresponds to the single receiver case that is given in the literature as (2), i.e., the union of Path 2 and Path 3 as if  $Rx_1$  is not in the environment. Therefore, if we calculate  $\alpha(t)$ , then we can calculate  $f_2^{Tx_1}(t)$ , which in turn will lead us to  $F_2^{Tx_1}(t)$ .

**Theorem 1.** The channel model functions in the case of two receivers (absorbing spheres), i.e.,  $F_1^{Tx_1}(t)$  and  $F_2^{Tx_1}(t)$ , are expressed in terms of four different single receiver channel model functions,  $G_1^{Tx_1}(t)$ ,  $G_2^{Tx_1}(t)$ ,  $G_1^{s'_1}(t)$ , and  $G_2^{s'_1}(t)$ , where  $s'_1$  and  $s'_2$  are points on  $Rx_1$  and  $Rx_2$ , respectively. Moreover,

$$F_2^{Tx_1}(t) = \frac{G_2^{Tx_1}(t) - G_2^{s'_1}(t)G_1^{Tx_1}(t)}{1 - G_2^{s'_1}(t)G_1^{s'_2}(t)} \quad (13)$$

$$F_1^{Tx_1}(t) = \frac{G_1^{Tx_1}(t) - G_1^{s'_2}(t)G_2^{Tx_1}(t)}{1 - G_2^{s'_1}(t)G_1^{s'_2}(t)}.$$

*Proof.* By definition, each of the molecules that is moving through Path 3 visits  $Rx_1$  at least once. Therefore, we can segment Path 3 into two parts. For those molecules originating from  $Tx_1$ , we denote the first hitting point on the surface of  $Rx_1$  as  $s_{1,Tx_1}$  and the corresponding first hitting time as  $\tau$ . Note that  $s_{1,Tx_1}$  can be an arbitrary point on the surface of  $Rx_1$  and  $\tau$  can be any real value less than  $t$ .

The instantaneous hitting probability density for  $s_{1,Tx_1}$  on the surface of  $Rx_1$  is denoted by  $f_1^{Tx_1}(t, s_{1,Tx_1})$ . Since  $s_{1,Tx_1}$  is the first hitting point on the surface of  $Rx_1$ , it can be regarded as the starting point of the successive path to  $Rx_2$ . Hence, (12) can be rewritten as

$$f_2^{Tx_1}(t) = g_2^{Tx_1}(t) - \int_0^t \int_{\Omega_1} f_1^{Tx_1}(\tau, s_{1,Tx_1}) g_2^{s_{1,Tx_1}}(t-\tau) ds_{1,Tx_1} d\tau, \quad (14)$$

where  $\Omega_1$  indicates the points on the surface of  $Rx_1$ . To obtain  $f_2^{Tx_1}(t)$ , we also need to consider  $f_1^{Tx_1}(t)$  in a similar way. Thus, we have the following:

$$f_1^{Tx_1}(t) = g_1^{Tx_1}(t) - \int_0^t \int_{\Omega_2} f_2^{Tx_1}(\tau, s_{2,Tx_1}) g_1^{s_{2,Tx_1}}(t-\tau) ds_{2,Tx_1} d\tau, \quad (15)$$

where  $s_{2,Tx_1}$  is the first hitting point on  $Rx_2$  that is analogous to  $s_{1,Tx_1}$  for  $Rx_1$ .

When we apply the mean value theorem for integration to the surface integration in (14), we get

$$f_2^{\text{Tx}_1}(t) = g_2^{\text{Tx}_1}(t) - \int_0^t g_2^{s'_1}(t-\tau) \int_{\Omega_1} f_1^{\text{Tx}_1}(\tau, s_{1,\text{Tx}_1}) ds_{1,\text{Tx}_1} d\tau, \quad (16)$$

where  $s'_1$  is a fixed point and by the mean value theorem, it can be found on the surface of  $\text{Rx}_1$ . After the surface integration in (16), we obtain

$$f_2^{\text{Tx}_1}(t) = g_2^{\text{Tx}_1}(t) - \int_0^t g_2^{s'_1}(t-\tau) f_1^{\text{Tx}_1}(\tau) d\tau. \quad (17)$$

Eq (17) is equivalent to saying that when molecules are absorbed by the non-intended receiver  $\text{Rx}_1$  before reaching the target receiver  $\text{Rx}_2$ , we can assume that all of those molecules will be absorbed by  $\text{Rx}_1$  at the same point  $s'_1$ . Hence,  $\exists s'_1 \in \Omega_1$  such that the following holds:

$$f_2^{\text{Tx}_1}(t) = g_2^{\text{Tx}_1}(t) - g_2^{s'_1}(t) * f_1^{\text{Tx}_1}(t), \quad (18)$$

where  $*$  is the convolution operator. Similarly,  $\exists s'_2 \in \Omega_2$  such that the following holds

$$f_1^{\text{Tx}_1}(t) = g_1^{\text{Tx}_1}(t) - g_1^{s'_2}(t) * f_2^{\text{Tx}_1}(t), \quad (19)$$

where  $s'_2$  is a fixed point on the surface of  $\text{Rx}_2$ . Using a property of convolution, by integrating (18) and (19), we have

$$F_2^{\text{Tx}_1}(t) = G_2^{\text{Tx}_1}(t) - G_2^{s'_1}(t) F_1^{\text{Tx}_1}(t) \quad (20)$$

$$F_1^{\text{Tx}_1}(t) = G_1^{\text{Tx}_1}(t) - G_1^{s'_2}(t) F_2^{\text{Tx}_1}(t). \quad (21)$$

By solving (20) and (21) simultaneously, we obtain

$$\begin{aligned} F_2^{\text{Tx}_1}(t) &= G_2^{\text{Tx}_1}(t) - G_2^{s'_1}(t) G_1^{\text{Tx}_1}(t) + G_2^{s'_1}(t) G_1^{s'_2}(t) F_2^{\text{Tx}_1}(t) \\ F_1^{\text{Tx}_1}(t) &= G_1^{\text{Tx}_1}(t) - G_1^{s'_2}(t) G_2^{\text{Tx}_1}(t) + G_2^{s'_1}(t) G_1^{s'_2}(t) F_1^{\text{Tx}_1}(t). \end{aligned} \quad (22)$$

Then, we get

$$\begin{aligned} F_2^{\text{Tx}_1}(t) &= \frac{G_2^{\text{Tx}_1}(t) - G_2^{s'_1}(t) G_1^{\text{Tx}_1}(t)}{1 - G_2^{s'_1}(t) G_1^{s'_2}(t)} \\ F_1^{\text{Tx}_1}(t) &= \frac{G_1^{\text{Tx}_1}(t) - G_1^{s'_2}(t) G_2^{\text{Tx}_1}(t)}{1 - G_2^{s'_1}(t) G_1^{s'_2}(t)}. \end{aligned} \quad (23)$$

□

After finding  $s'_1$  and  $s'_2$  numerically, we can calculate (23) by using (2). Then, we can formulate the BER in terms of the following probabilities

$$\begin{aligned} P_{12}[k] &= F_2^{\text{Tx}_1}((k+1)t_s) - F_2^{\text{Tx}_1}(kt_s) \\ P_{11}[k] &= F_1^{\text{Tx}_1}((k+1)t_s) - F_1^{\text{Tx}_1}(kt_s). \end{aligned} \quad (24)$$

TABLE I  
SIMULATION PARAMETERS FOR CHANNEL MODEL VERIFICATION

System Parameter	Notation	Values
Distance	$d_1=d_2$	1.5 $\mu\text{m}$ , 2 $\mu\text{m}$
Distance	$d_{\text{Tx}_1}^{\text{Rx}_2}=d_{\text{Tx}_2}^{\text{Rx}_1}$	5 $\mu\text{m}-d_1$
Number of Molecules for Bit 1	$N_1$	50000
Diffusion Coefficient	D	100 $\mu\text{m}^2/\text{s}$
Radius of Receiver	$r_{r1}=r_{r2}$	5 $\mu\text{m}$
Simulation Time Step	$\Delta t$	$10^{-5}\text{s}$
Simulation Duration		0.1 s
Simulation Replication		5

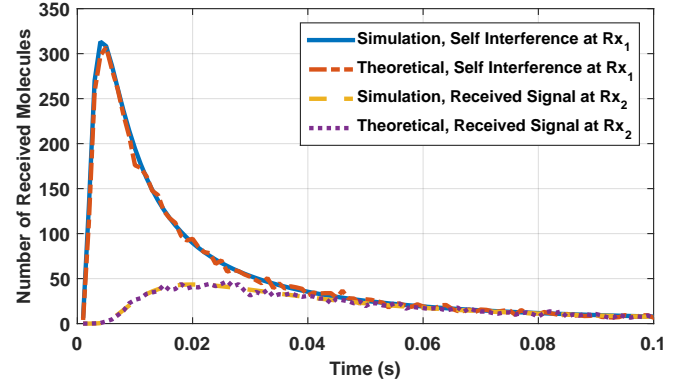


Fig. 6. A comparison of the theoretical number of received molecules with the simulation data ( $d_1=d_2=1.5 \mu\text{m}$ ).

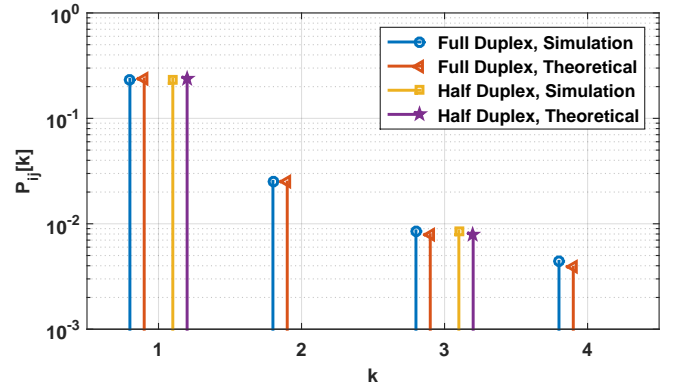


Fig. 7. A comparison of the theoretical channel coefficients with the simulation data ( $t_s = 0.150\text{s}$ ,  $d_1=d_2=1.5 \mu\text{m}$ ,  $r_{r1}=r_{r2}=5 \mu\text{m}$ ).

## B. Channel Model Verification

The derived two-way MCvD system channel model has two unknown coefficients,  $s'_1$  and  $s'_2$ . We find  $s'_1$  and  $s'_2$  by using a numerical method and compare the proposed channel model with the simulation results. In each simulated trial, 50000 molecules are released, and we take the mean value of the number of received molecules. The received molecules are distinguished according to the transmitter that emits them. For simplicity in simulations, only  $\text{Tx}_1$  releases molecules which is sufficient to verify the theoretical channel model.

To implement Brownian motion for the emitted molecules, our simulator records and updates the position of each molecule at each time step  $\Delta t$ . The position of the emitted

TABLE II  
RMSE VALUES BETWEEN THEORETICAL MODEL AND SIMULATION RESULTS

System Parameter	Formula	RMSE	
		Proposed Model	Previous Model [27]
$d_1=d_2=1.5\ \mu\text{m}$	$F_1^{\text{Tx}_1}(t)$	$1.90 \times 10^{-3}$	$3.33 \times 10^{-2}$
	$F_2^{\text{Tx}_1}(t)$	$4.00 \times 10^{-3}$	$3.73 \times 10^{-2}$
$d_1=d_2=2\ \mu\text{m}$	$F_1^{\text{Tx}_1}(t)$	$2.7 \times 10^{-3}$	$4.04 \times 10^{-2}$
	$F_2^{\text{Tx}_1}(t)$	$3.4 \times 10^{-3}$	$4.01 \times 10^{-2}$

molecules,  $\mathbf{X}_p(t)$ , changes by  $\Delta\mathbf{X}_p$  after simulation time step  $\Delta t$  as in (25) [29]. The simulation parameters used for verification of the channel model are given in Table I.

$$\begin{aligned} \mathbf{X}_p(t + \Delta t) &= \mathbf{X}_p(t) + \Delta\mathbf{X}_p \\ &= \mathbf{X}_p(t) + (\Delta x, \Delta y, \Delta z) \quad (25) \\ \Delta x, \Delta y, \Delta z &\sim \mathcal{N}(0, 2D\Delta t). \end{aligned}$$

Through extensive simulations, we obtain the number of received molecules for each receiver (i.e.,  $\text{Rx}_1$  and  $\text{Rx}_2$ ) at each time step during the simulation time, i.e.,  $F_{2,\text{sim}}^{\text{Tx}_1}(t)$  and  $F_{1,\text{sim}}^{\text{Tx}_1}(t)$ , respectively. Then, we use (23) to calculate  $F_2^{\text{Tx}_1}(t)$  and  $F_1^{\text{Tx}_1}(t)$ . Next, we compare the analytical results with the simulation results, as shown in Fig. 6. Furthermore, we compare the channel coefficients in case of both half-duplex and full-duplex systems (see Fig. 7).

To verify the derived channel model, we evaluate the root-mean-square error (RMSE) between  $F_i^{\text{Tx}_1}(t)$  and  $F_{i,\text{sim}}^{\text{Tx}_1}(t)$  as follows:

$$\text{RMSE}(F_i^{\text{Tx}_1}(t)) = \sum_{t \in \mathcal{T}} \sqrt{\frac{(F_i^{\text{Tx}_1}(t) - F_{i,\text{sim}}^{\text{Tx}_1}(t))^2}{|\mathcal{T}|}}, \quad (26)$$

where  $\mathcal{T}$  is the set of time samples and  $|\cdot|$  is the cardinality of a set. The elements of  $\mathcal{T}$  are selected according to the simulation end time. Also, we evaluate the RMSE between the channel model in [27] and  $F_{i,\text{sim}}^{\text{Tx}_1}(t)$  to compare with  $F_i^{\text{Tx}_1}(t)$  (see Table II).

### C. BER Formula for Two-Way Molecular Communication

To complete the BER formula, we substitute  $P_{ij}(t_1, t_2)$  using  $F_j^{\text{Tx}_i}(t)$  as follows:

$$\begin{aligned} P_{ij}(t_1, t_2) &= F_j^{\text{Tx}_i}(t_2) - F_j^{\text{Tx}_i}(t_1) \\ P_{ij}[k] &= F_j^{\text{Tx}_i}((k+1)t_s) - F_j^{\text{Tx}_i}(kt_s). \quad (27) \end{aligned}$$

Now, we can formulate the BER in terms of the Q-function (i.e., the tail probability of the standard normal distribution). For the receiver  $\text{Rx}_j$ , an error occurs when the result of decoding is different from the bit transmitted from the  $\text{Tx}_i$ . If  $\text{Tx}_i$  encodes bit-1, an error occurs when  $y_{\text{Rx}_j}[n]$  is less than the detection threshold  $\tau_t$ . If  $\text{Tx}_i$  encodes bit-0, then an error occurs when  $y_{\text{Rx}_j}[n]$  is greater than the detection threshold  $\tau_t$ . Considering the transmitted bit sequences  $x_i$  and  $x_j$ , we obtain the error probabilities at the  $n^{\text{th}}$  symbol slot as (28)

TABLE III  
SIMULATION PARAMETERS FOR BER AND THROUGHPUT COMPARISON

System Parameter	Notation	Values
Distance	$d_1=d_2$	1.5 $\mu\text{m}$
Distance	$d_{\text{Tx}_2}^{\text{Rx}_1}=d_{\text{Tx}_1}^{\text{Rx}_2}$	5 $\mu\text{m}-d_1$
Number of Molecules for Bit 1	$N_1$	300, 400, 500
Diffusion Coefficient	$D$	100 $\mu\text{m}^2/\text{s}$
Radius of Receiver	$r_r$	5 $\mu\text{m}$
Simulation Time Step	$\Delta t$	$10^{-5}\text{s}$
Molecular Noise Variance	$\sigma_{\text{noise}}^2$	100
Considered ISI Period		0.6s
Replication		5

where  $x_i[1:n-1]$  denotes the bits transmitted previously from  $\text{Tx}_i$ :

$$\begin{aligned} P_e^{j,BSCK} &= P_{e,x_i[n]=1}^{j,BSCK} + P_{e,x_i[n]=0}^{j,BSCK} \\ &= \sum_{x_i[1:n-1], x_j[1:n]} P_{i,1} P(y_{\text{Rx}_j}[n] \leq \tau_t | x_i[n]=1, x_i, x_j) \\ &\quad + \sum_{x_i[1:n-1], x_j[1:n]} P_{i,0} P(y_{\text{Rx}_j}[n] > \tau_t | x_i[n]=0, x_i, x_j) \\ &= \sum_{x_i[1:n-1], x_j[1:n]} P_{i,1} Q\left(\frac{\mu_{\text{total}}|x_i, x_j - \tau_t}{\sigma_{\text{total}}^2|x_i, x_j}\right) \\ &\quad + \sum_{x_i[1:n-1], x_j[1:n]} P_{i,0} Q\left(\frac{\tau_t - \mu_{\text{total}}|x_i, x_j}{\sigma_{\text{total}}^2|x_i, x_j}\right), \quad (28) \end{aligned}$$

where  $\mu_{\text{total}}$  is defined in (7),  $Q(\cdot)$  is the Q-function, and

$$\begin{aligned} P_{i,1} &= P(x_i[n]=1) P(x_i[1:n-1]) P(x_j[1:n]) \\ P_{i,0} &= P(x_i[n]=0) P(x_i[1:n-1]) P(x_j[1:n]). \quad (29) \end{aligned}$$

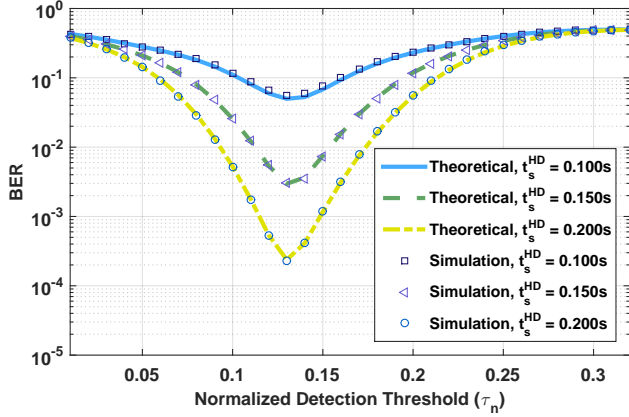
## V. NUMERICAL RESULTS

In this section, we compare the proposed half-duplex and full-duplex systems in terms of BER and throughput. Throughput of the systems are evaluated as follows:

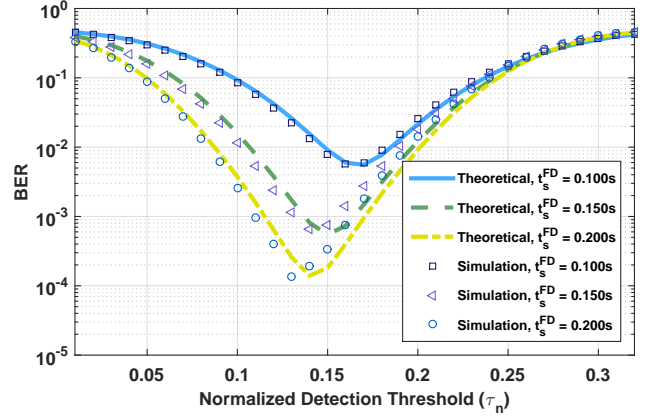
$$\text{Throughput} = \frac{M(1 - P_e)}{t_s}, \quad (30)$$

where  $M$  is the number of bits transmitted in one symbol,  $P_e$  is the BER of the system, and  $t_s$  denotes the symbol duration. The system parameters for the rest of our work are summarized in Table III. For convenience, we denote  $t_s$  of the half-duplex and full-duplex systems as  $t_s^{\text{HD}}$  and  $t_s^{\text{FD}}$ , respectively.

In the half-duplex system, each receiver operates only when the paired transmitter releases the molecular signal. Hence, the operating time of the receiver (i.e., detection period) is half of the symbol duration. In the full-duplex system, the detection period of each receiver is equal to the symbol duration. Roughly, we can expect faster but less accurate communications in the full-duplex system if we use the same modulation technique and detection period for both systems. By the theoretical and simulation BER analysis, we confirm that the proposed SIC techniques are necessary in the full-duplex system. Therefore we analyze the BER improvement in the full-duplex system with SIC to find, numerically, the



(a) Half-duplex system



(b) Full-duplex

Fig. 8. (a) BER comparison of the simulation data and the theoretical analysis of the half-duplex system using BCSK (b) BER comparison of the simulation data and the theoretical analysis of the full-duplex system with DSIC ( $N_1=500$ ,  $d_1=d_2=1.5 \mu\text{m}$ ,  $r_{r1}=r_{r2}=5 \mu\text{m}$ ).

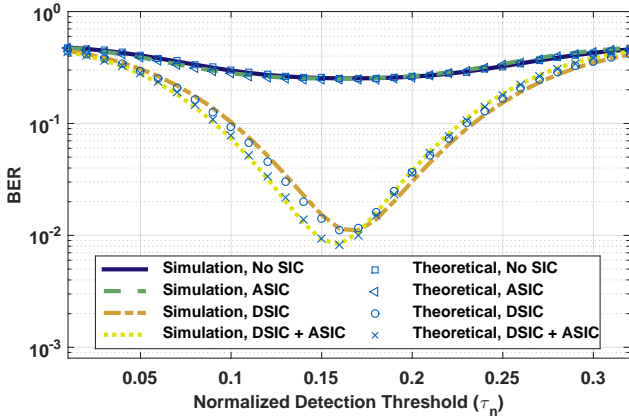


Fig. 9. BER of the full-duplex system with the different SIC techniques ( $N_1=500$ ,  $t_s^{\text{FD}}=0.1\text{s}$ ,  $d_1=d_2=1.5 \mu\text{m}$ ,  $r_{r1}=r_{r2}=5 \mu\text{m}$ ).

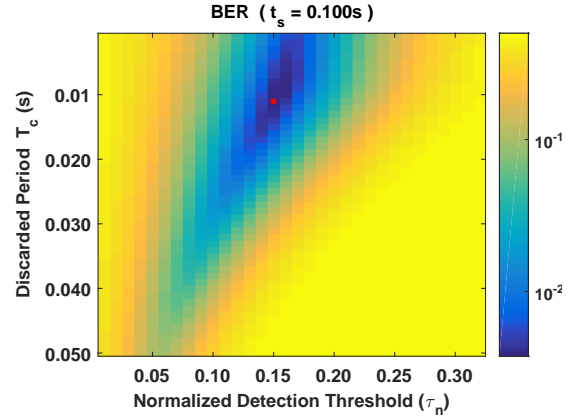


Fig. 10. Theoretical BER heatmap of the full-duplex system with ASIC and DSIC. The red marks indicate the optimal parameters for the normalized detection threshold and the discarded period.

optimal values for the normalized detection threshold and the time after which molecules are discarded period of the SIC to minimize BER. Through the numerical parameter optimization, the throughput of the full-duplex system with SIC is compared to the half-duplex system. For a fair comparison, we evaluate the throughput in the following three cases, considering that the throughput is a function of  $M$ ,  $t_s$ , and  $P_e$ :

- 1) Half-duplex system (BCSK) vs. full-duplex system (BCSK) with SIC, where  $t_s^{\text{FD}} = t_s^{\text{HD}}/2$ .
- 2) Half-duplex system (BCSK) vs. full-duplex system (BCSK) with SIC. We set the same  $t_s$  for both systems (i.e.,  $t_s^{\text{FD}} = t_s^{\text{HD}}$ ).
- 3) Half-duplex system (BCSK) vs. full-duplex system (BCSK) with SIC. We empirically adjust  $t_s^{\text{FD}}$  to make the BER of both systems the same level.
- 4) Half-duplex system using quadrature concentration shift keying (QCSK) vs full-duplex system (BCSK) with SIC, where  $t_s^{\text{FD}} = t_s^{\text{HD}}/2$ .

#### A. BER Analysis

Fig. 8(a) depicts the simulation and theoretical BERs of the half-duplex system using BCSK. The  $x$ -axis is the normalized threshold ( $\tau_n$ ), which is  $\tau_t/N_1$ . First of all, the simulation and theoretical values match each other well. Since the half-duplex system is not susceptible to SI, we do not need to apply the proposed SIC techniques to this system. On the other hand, we observe from Fig. 9 that the BER of the full-duplex system is nearly 0.3 if we do not apply the SIC techniques. In Fig. 8(a), we can see the optimal normalized threshold  $\tau_n^*$  for different  $t_s^{\text{HD}}$  and we observe that it is slightly changing according to the value of  $t_s^{\text{HD}}$ . We also observe that the BER gain is relatively higher for changing  $t_s^{\text{HD}}$  from 0.100s to 0.150s compared to from 0.150s to 0.200s due to the relative ISI difference.

Fig. 8(b) shows the simulation and theoretical BER of the full-duplex system with DSIC. We can see that there is an optimal normalized detection threshold  $\tau_n^*$  for different  $t_s^{\text{FD}}$  values. Similar to the case of the half-duplex system, there is some similarity between the  $\tau_n^*$  changes according to the  $t_s^{\text{FD}}$



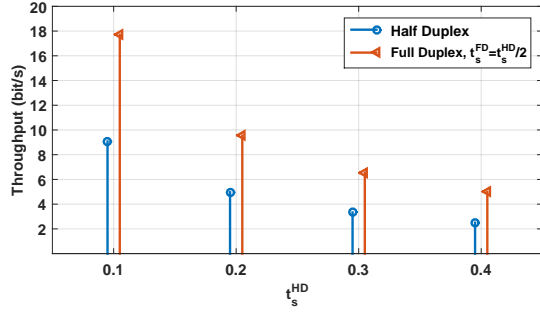
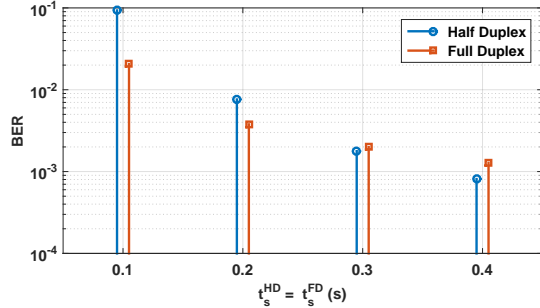
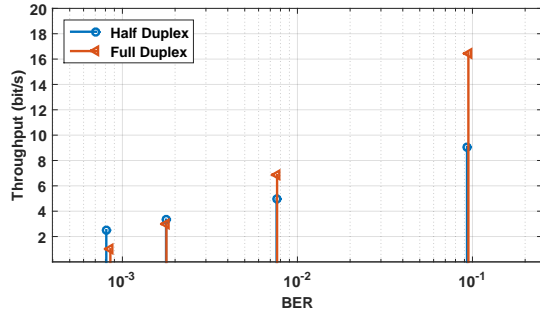
(a)  $t_s^{\text{FD}} = t_s^{\text{HD}}/2$ ,  $N_1=300$ (b) set  $t_s$ ,  $N_1=300$ (c) set BER,  $N_1=300$ 

Fig. 11. (a) Theoretical BER of the half-duplex system (BCSK) and the full-duplex system with optimized DSIC and ASIC (BCSK) where  $t_s^{\text{FD}} = t_s^{\text{HD}}/2$ , (b)  $t_s^{\text{FD}} = t_s^{\text{HD}}$ . (c) We adjust  $t_s^{\text{FD}}$  as per Table IV to make the BER of both systems the same level and compare the throughput. When  $N_1$  is 400 or 500 and  $t_s^{\text{HD}}$  is 0.400 s, it is infeasible to make their BER the same.

value and also the tendency of the BER gain with respect to the  $t_s^{\text{FD}}$  difference (see Fig. 8(a)).

Fig. 9 depicts the simulation and theoretical BERs of the full-duplex system while applying the different SIC techniques. The  $x$ -axis is the normalized detection threshold  $\tau_t/N_1$ . We observe that the BER of the full-duplex system with ASIC is nearly 0.3. On the other hand, the BER of the full-duplex system with DSIC becomes comparable with the half-duplex system in Fig.8(a). Moreover, we observe that if we apply both SIC techniques, the BER is slightly improved compared to the full-duplex system with only DSIC. For the full-duplex systems, since the performances of the ASIC-only system and the no-SIC system are not at reasonable BER levels, we consider those full-duplex systems with only DSIC or DSIC and ASIC.

As derived in Section IV, the BER is a function of symbol

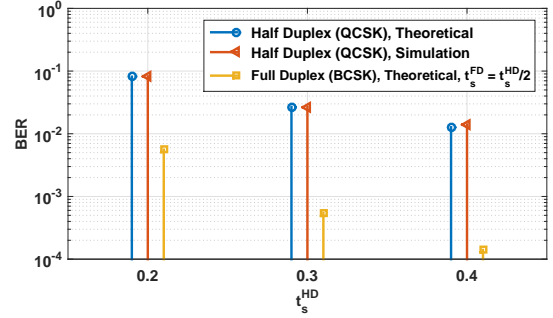


Fig. 12. Theoretical and simulation BER of the half-duplex system (QCSK) and the theoretical BER of the full-duplex system with optimized DSIC and ASIC (BCSK),  $N_1$  is 500.

duration ( $t_s$ ), detection threshold ( $\tau_t$ ), the number of molecules for encoding bit-1 ( $N_1$ ), and the discarded period of molecular received signal for ASIC ( $T_c$ ). Since  $N_1$  and  $t_s$  are system parameters, we consider only  $\tau_t$  and  $T_c$  as variables to optimize. While we will show that optimal values for these parameters exist, we cannot derive them in closed-form and hence must resort to evaluating them numerically. To improve BER, we first need to see the structure of the BER of the full-duplex system with SIC in terms of  $\tau_t$  and  $T_c$  by the following analysis.

In Fig. 10, we depict a heatmap of the theoretical BER with respect to  $T_c$  and  $\tau_n$  for the full-duplex system with DSIC and ASIC. We observe that there is an optimal  $T_c$  to minimize the BER for the given  $t_s^{\text{FD}}$ . For each  $t_s^{\text{FD}}$ , we find global optimal normalized detection threshold and the time after which molecules are discarded period in order to minimize the BER and denote them as red marks on the heatmap. We utilized these optimal values in the SIC algorithm to compare the throughput of the half-duplex system and the full-duplex system with SIC.

As was mentioned before, for comparison, we consider the following three cases: i) set  $t_s^{\text{FD}} = t_s^{\text{HD}}/2$  (to observe a trade off between the throughput and BER); ii) set the same  $t_s$  for both systems; iii) fix  $t_s^{\text{HD}}$  and adjust  $t_s^{\text{FD}}$  empirically to make the BER of both systems the same level. Figs. 11(a), 11(b) and 11(c) correspond to cases i), ii) and iii), respectively. For the case ii), adjusted  $t_s^{\text{FD}}$  values are in Table IV.

For the case i), Fig. 11(a) shows that the throughputs of the full-duplex system with optimized SIC are almost double the throughput of the half-duplex system. Thus, we can achieve nearly double the transmission rate using the proposed SIC techniques without degrading the BER significantly. When  $t_s^{\text{HD}} = t_s^{\text{FD}}$  is 0.100 s or 0.200 s, the BER of the full-duplex system with optimized SIC is less than the BER of the half-duplex system. The converse is true when  $t_s^{\text{HD}} = t_s^{\text{FD}}$  is 0.300 s or 0.400 s. Adjusted  $t_s^{\text{FD}}$  throughput values in Table IV show the same tendency. The overall results imply that if the communication constraint is focused on throughput, the full-duplex system with optimized SIC is better than the half-duplex system even in terms of BER.

In Fig. 12 we depict the simulation and theoretical BER of the half-duplex system using QCSK and compare them

TABLE IV

THROUGHPUT RATIO (FD/HD),  $t_s$  AND BER VALUES OF THE HALF-DUPLEX SYSTEM USING BCSK AND THE FULL-DUPLEX SYSTEM USING BCSK.

		$N_1 = 300$				$N_1 = 400$				$N_1 = 500$			
Case 1	$t_s^{\text{HD}} = 2t_s^{\text{FD}}$	0.100 s	0.200 s	0.300 s	0.400 s	0.100 s	0.200 s	0.300 s	0.400 s	0.100 s	0.200 s	0.300 s	0.400 s
	BER (FD)	0.1149	0.0206	0.0071	0.0038	0.0881	0.0083	0.0017	0.0006	0.0474	$2.4 \times 10^{-4}$	$1 \times 10^{-5}$	$2 \times 10^{-6}$
	BER (HD)	0.0931	0.0076	0.0018	0.0008	0.0665	0.0014	0.0001	$3 \times 10^{-5}$	0.0498	$2.3 \times 10^{-4}$	$9 \times 10^{-6}$	$9 \times 10^{-7}$
	THP Ratio	1.951	1.973	1.989	1.994	1.953	1.986	1.996	1.998	2.005	1.999	1.999	1.999
Case 2	$t_s^{\text{FD}} = t_s^{\text{HD}}$	0.100 s	0.200 s	0.300 s	0.400 s	0.100 s	0.200 s	0.300 s	0.400 s	0.100 s	0.200 s	0.300 s	0.400 s
	BER (FD)	0.0206	0.0038	0.0020	0.0013	0.0084	0.0006	0.0002	0.0001	0.0038	0.0001	$3.3 \times 10^{-5}$	$1 \times 10^{-5}$
	BER (HD)	0.0931	0.0076	0.0018	0.0008	0.0665	0.0014	0.0001	$3.6 \times 10^{-5}$	0.0498	$2.3 \times 10^{-4}$	$9 \times 10^{-6}$	$9 \times 10^{-7}$
	THP Ratio	1.0800	1.0039	0.9998	0.9995	1.0623	1.0007	0.9999	0.9999	1.0485	1.0001	0.9999	0.9999
Case 3	$t_s^{\text{HD}}$	0.100 s	0.200 s	0.300 s	0.400 s	0.100 s	0.200 s	0.300 s	0.400 s	0.100 s	0.200 s	0.300 s	0.400 s
	$t_s^{\text{FD}}$	0.055 s	0.145 s	0.330 s	1 s	0.057 s	0.163 s	0.400 s	N/A	0.057 s	0.173 s	0.400 s	N/A
	THP Ratio	1.814	1.379	0.909	0.400	1.763	1.227	0.750	N/A	1.822	1.379	0.901	N/A

TABLE V

THROUGHPUT RATIO (FD/HD) OF THE HALF-DUPLEX SYSTEM USING QCSK AND THE FULL-DUPLEX SYSTEM USING BCSK WITH OPTIMIZED DSIC AND ASIC

$N_1$	$t_s^{\text{HD}}$ (s)	$t_s^{\text{FD}}$ (s)	Throughput Ratio (FD/HD)
300	0.200	0.100	1.112
	0.300	0.150	1.052
	0.400	0.200	1.032
400	0.200	0.100	1.096
	0.300	0.150	1.037
	0.400	0.200	1.020
300	0.200	0.100	1.082
	0.300	0.150	1.027
	0.400	0.200	1.012

to the full-duplex system with optimized SIC using BCSK where  $t_s^{\text{FD}} = t_s^{\text{HD}}/2$ . In this case,  $M/t_s$  is the same for both systems. Hence, the BER determines the difference between the throughputs. For QCSK, we used an equally spaced number of molecules for encoding different bits (i.e., bit-0, 1, 2, 3) and three thresholds (i.e.,  $\tau_{t1}$ ,  $\tau_{t2}$ ,  $\tau_{t3}$ ) to detect the molecular received signal. Fig. 12 shows that the BER of the half-duplex system using QCSK is much higher than that of the full-duplex system using BCSK with optimized SIC. The BER formula of the half-duplex system using QCSK is (31) in Appendix A. The throughput difference between the two systems can be seen in Table V.

## VI. CONCLUSION

We have investigated two different communication models of two-way MCvD—a half-duplex system and a full-duplex system. We proposed a new approach to derive the model of the impulse response of a multi-receiver channel model. We also derived the BER formula and verified the formula by simulation. Theoretical analysis and simulations showed that severe SI occurs in the full-duplex system. Therefore, we proposed two SIC techniques to mitigate this interference: ASIC and DSIC. We analyzed the BER improvements in the full-duplex system with the proposed SIC techniques and numerically found the optimal values for the normalized detection threshold and the time after which molecules are discarded period in order to minimize the system BER. To compare the

half-duplex system with the full-duplex system, we evaluated the throughput in three different cases. The throughput of the full-duplex system with optimized SIC increased to more than that of the half-duplex system as  $t_s$  decreased. With the proposed SIC techniques, we showed the possibility of full-duplex molecular communication using a single type of molecule. On the other hand, the BER analysis and simulation results revealed that using a concentration-based modulation technique of higher order significantly degrades the BER. Investigating a more effective modulation technique for the two-way MCvD will be a topic for the future work.

## APPENDIX

### A. BER Formula (QCSK)

BER formulations of the half-duplex and full-duplex systems for QCSK are

$$\begin{aligned}
P_e^{j,QCSK} &= P_{e,x_i[n]=3}^{j,QCSK} + P_{e,x_i[n]=2}^{j,QCSK} + P_{e,x_i[n]=1}^{j,QCSK} + P_{e,x_i[n]=0}^{j,QCSK} \\
&= \sum_{x_i[1:n-1], x_j[1:n]} P_{i,3} P(y_{\text{Rx}_j}[n] \leq \tau_{t3} | x_i[n]=3, x_i, x_j) \\
&\quad + \sum_{x_i[1:n-1], x_j[1:n]} P_{i,2} P(y_{\text{Rx}_j}[n] \leq \tau_{t2} | x_i[n]=2, x_i, x_j) \\
&\quad + \sum_{x_i[1:n-1], x_j[1:n]} P_{i,2} P(\tau_{t3} < y_{\text{Rx}_j}[n] | x_i[n]=2, x_i, x_j) \\
&\quad + \sum_{x_i[1:n-1], x_j[1:n]} P_{i,1} P(y_{\text{Rx}_j}[n] \leq \tau_{t1} | x_i[n]=1, x_i, x_j) \\
&\quad + \sum_{x_i[1:n-1], x_j[1:n]} P_{i,1} P(\tau_{t2} < y_{\text{Rx}_j}[n] | x_i[n]=1, x_i, x_j) \\
&\quad + \sum_{x_i[1:n-1], x_j[1:n]} P_{i,0} P(y_{\text{Rx}_j}[n] > \tau_{t1} | x_i[n]=0, x_i, x_j) \\
&= \sum_{x_i[1:n-1], x_j[1:n]} P_{i,3} Q \left( \frac{\mu_{\text{total}} | x_i, x_j - \tau_{t3}}{\sigma_{\text{total}}^2 | x_i, x_j} \right) \\
&\quad + \sum_{x_i[1:n-1], x_j[1:n]} P_{i,2} Q \left( \frac{\mu_{\text{total}} | x_i, x_j - \tau_{t2}}{\sigma_{\text{total}}^2 | x_i, x_j} \right) \\
&\quad + \sum_{x_i[1:n-1], x_j[1:n]} P_{i,2} Q \left( \frac{\tau_{t3} - \mu_{\text{total}} | x_i, x_j}{\sigma_{\text{total}}^2 | x_i, x_j} \right)
\end{aligned}$$

$$\begin{aligned}
& + \sum_{x_i[1:n-1], x_j[1:n]} P_{i,1} Q \left( \frac{\mu_{\text{total}}|x_i, x_j - \tau t_1}{\sigma_{\text{total}}^2|x_i, x_j} \right) \\
& + \sum_{x_i[1:n-1], x_j[1:n]} P_{i,1} Q \left( \frac{\tau t_2 - \mu_{\text{total}}|x_i, x_j}{\sigma_{\text{total}}^2|x_i, x_j} \right) \\
& + \sum_{x_i[1:n-1], x_j[1:n]} P_{i,0} Q \left( \frac{\tau t_1 - \mu_{\text{total}}|x_i, x_j}{\sigma_{\text{total}}^2|x_i, x_j} \right), \quad (31)
\end{aligned}$$

where  $Q(\cdot)$  is the Q-function and

$$P_{i,k} = P(x_i[n]=k) P(x_i[1:n-1]) P(x_j[1:n]). \quad (32)$$

## REFERENCES

- [1] D. A. LaVan, T. McGuire, and R. Langer, "Small-scale systems for in vivo drug delivery," *Nat. Biotechnol.*, vol. 21, no. 10, pp. 1184–1191, Oct. 2003.
- [2] A. A. G. Requicha, "Nanorobots, NEMS, and nanoassembly," *Proc. IEEE*, vol. 91, no. 11, pp. 1922–1933, Nov. 2003.
- [3] S. Basu, Y. Gerchman, C. H. Collins, F. H. Arnold, and R. Weiss, "A synthetic multicellular system for programmed pattern formation," *Nature*, vol. 434, no. 7037, pp. 1130–1134, Apr. 2005.
- [4] A. Cavalcanti and R. A. Freitas-Jr., "Nanorobotics control design: a collective behavior approach for medicine," *IEEE Trans. Nanobiosci.*, vol. 4, no. 2, pp. 133–140, Jun. 2005.
- [5] P. Couvreur and C. Vauthier, "Nanotechnology: Intelligent design to treat complex disease," *Springer Pharmaceut. Res.*, vol. 23, no. 7, pp. 1417–1450, Jun. 2006.
- [6] N. Farsad, H. B. Yilmaz, A. Eckford, C.-B. Chae, and W. Guo, "A comprehensive survey of recent advancements in molecular communication," *IEEE Commun. Surveys Tuts.*, vol. 18, no. 3, pp. 1887–1919, Oct. 2016.
- [7] W. Guo, C. Mias, N. Farsad, and J.-L. Wu, "Molecular versus electromagnetic wave propagation loss in macro-scale environments," *IEEE Trans. Mol. Biol. Multi-Scale Commun.*, vol. 1, no. 1, pp. 18–25, Mar. 2015.
- [8] D. Malak and O. B. Akan, "Molecular communication nanonetworks inside human body," *Elsevier Nano Commun. Netw.*, vol. 3, no. 1, pp. 19–35, Mar. 2012.
- [9] M. S. Kuran, H. B. Yilmaz, T. Tugcu, and B. zerman, "Energy model for communication via diffusion in nanonetworks," *Nano Communication Networks*, vol. 1, no. 2, Jul. 2010.
- [10] S. Redner, *A guide to first-passage processes*. Cambridge University Press, Aug. 2001.
- [11] K. V. Srinivas, A. W. Eckford, and R. S. Adve, "Molecular communication in fluid media: The additive inverse gaussian noise channel," *IEEE Trans. Inf. Theory*, vol. 58, no. 7, pp. 4678–4692, Dec. 2012.
- [12] T. Nakano, Y. Okaie, and J.-Q. Liu, "Channel model and capacity analysis of molecular communication with brownian motion," *IEEE Commun. Lett.*, vol. 16, no. 6, pp. 797–800, Jun. 2012.
- [13] H. B. Yilmaz, A. C. Heren, T. Tugcu, and C.-B. Chae, "Three-dimensional channel characteristics for molecular communications with an absorbing receiver," *IEEE Commun. Lett.*, vol. 18, no. 6, pp. 929–932, Apr. 2014.
- [14] G. Genc, Y. E. Kara, H. B. Yilmaz, and T. Tugcu, "ISI-aware modeling and achievable rate analysis of the diffusion channel," *IEEE Commun. Lett.*, vol. 20, no. 9, pp. 1729–1732, Jun. 2016.
- [15] A. Noel, K. C. Cheung, and R. Schober, "Improving receiver performance of diffusive molecular communication with enzymes," *IEEE Trans. Nanobiosci.*, vol. 13, no. 1, pp. 31–43, Mar. 2014.
- [16] Y. J. Cho, H. Birkan Yilmaz, W. Guo, and C.-B. Chae, "Effective enzyme deployment for degradation of interference molecules in molecular communication," *IEEE Trans. on Emerging Tel. Tech.*, vol. 28, no. 7, pp. 1–12, Apr. 2017.
- [17] B. Tepekule, A. E. Pusane, H. B. Yilmaz, C.-B. Chae, and T. Tugcu, "ISI mitigation techniques in molecular communication," *IEEE Trans. Mol. Biol. Multi-Scale Commun.*, vol. 1, no. 2, pp. 202–216, Jun. 2015.
- [18] A. E. P. Bayram Cevdet Akdeniz and T. Tugcu, "Two-way communication systems in molecular communication," in *Proc. IEEE Int. Black Sea Conf. on Commun. and Netw. (BlackSeaCom)*, Jun. 2017.
- [19] Y. Huang, M. Wen, C. Lee, C.-B. Chae, and F. Ji, "Two-way molecular communications assisted with an impulsive flow," to appear in *IEEE Trans. Ind. Informat.*, doi: 10.1109/TII.2019.2897066, 2019.
- [20] N.-R. Kim and C.-B. Chae, "Novel modulation techniques using isomers as messenger molecules for nano communication networks via diffusion," *IEEE J. Sel. Areas Commun.*, vol. 31, no. 12, pp. 847–856, Dec. 2013.
- [21] N.-R. Kim, A. Eckford, and C.-B. Chae, "Symbol interval optimization for molecular communication with drift," *IEEE Trans. Nanotechnol.*, vol. 13, no. 3, pp. 223–229, Jul. 2014.
- [22] N.-R. Kim, N. Farsad, A. Eckford, and C.-B. Chae, "Channel and noise models for nonlinear molecular communication systems," *IEEE J. Sel. Areas Commun.*, vol. 32, no. 12, pp. 2392–2401, Dec. 2014.
- [23] N. Farsad, W. Guo, and A. Eckford, "Tabletop molecular communication: Text messages through chemical signals," *PLoS one*, vol. 8, no. 12, p. e82935, Dec. 2013.
- [24] H. ShahMohammadian, G. G. Messier, and S. Magierowski, "Blind synchronization in diffusion-based molecular communication channels," *IEEE Commun. Lett.*, vol. 17, no. 11, pp. 2156–2159, Nov. 2013.
- [25] M. S. Kuran, H. B. Yilmaz, T. Tugcu, and I. F. Akyildiz, "Modulation techniques for communication via diffusion in nanonetworks," in *Proc. IEEE Int. Conf. on Commun. (ICC)*, Jun. 2011, pp. 1–5.
- [26] H. B. Yilmaz and C.-B. Chae, "Arrival modeling for molecular communication via diffusion," *Electronics Letters*, vol. 50, no. 23, pp. 1667–1669, Oct. 2014.
- [27] B. H. Koo, C. Lee, H. B. Yilmaz, N. Farsad, A. Eckford, and C. B. Chae, "Molecular MIMO: From theory to prototype," *IEEE J. Sel. Areas Commun.*, vol. 34, no. 3, pp. 600–614, Mar. 2016.
- [28] C. Lee, H. B. Yilmaz, C.-B. Chae, N. Farsad, and A. Goldsmith, "Machine learning based channel modeling for molecular MIMO communications," in *Proc. IEEE Workshop on Signal Process. Adv. in Wireless Commun. (SPAWC)*, Apr. 2017.
- [29] H. B. Yilmaz and C.-B. Chae, "Simulation study of molecular communication systems with an absorbing receiver: Modulation and ISI mitigation techniques," *Simulation Modelling Practice and Theory*, vol. 49, pp. 136–150, Dec. 2014.